Lasers in Manufacturing Conference 2017

Effect of material gauge on laser weld pool mixing between dissimilar steels

A. Métais[a,b,*], P. Sallamand[a], I. Tomashchuk[a], S. Gaied[b]

[a] *Laboratoire Interdisciplinaire Carnot de Bourgogne (ICB), UMR 6303 CNRS / Université de Bourgogne Franche-Comté, 12 rue de la fonderie, 71200 Le Creusot, France*

[b] *ArcelorMittal, Global R&D Montataire, 1 route de Saint Leu, 60761 Montataire, France*

Abstract

Welding dissimilar steels offers a great potential to increase safety and/or decrease the weight of cars while at the same time reducing their cost. Thickness and grades have to be optimized to decrease weight of vehicle, but safety is also assured by the quality of the joint. Thus, the prediction of the local chemical composition in the weld is essential to determine the mechanical behavior of the weld.

The goal of the present paper is to present the effect of the thickness ratio on laser weld pool mixing between dissimilar steels. Numerical results are obtained by a multiphysical model (including heat transfer, turbulent flow and transport of species) developed within COMSOL Multiphysics finite element software. In order to validate the developed model, SEM-EDX analyses on experimental cross-sections have been performed to obtain quantitative mapping of elements distributions in the melted zone. The comparison shows a good agreement between numerical model and experimental data.

Keywords: Laser welding ; dissimilar materials ; melt pool ; mixing ; different thickness

1. Introduction

Tailored Welded Blanks (TWBs) are useful for reducing car weight because they enable economical design of joined parts with good balance between design stress and material strength. The influence of thickness ratio of tailored welded blanks on their properties was discussed only in few publications: Seto et al, 2007

* Corresponding author. Tel.: +3-338-573-1017
E-mail address: alexandre.metais@arcelormittal.com

reported on fatigue properties of such joints and recently Safdarian et al, 2013 and Song et al, 2014 studied their formability. Nevertheless, the influence of thickness ratio on mixing process in the melt pool and on tensile properties is not yet studied for a case of laser welding of dissimilar materials. It is known that alloying elements dilution during laser welding of dissimilar materials strongly influences final tensile properties of the weld. In present study, previously developed numerical model (Métais et al, 2016[a]), that describes mixing of melted materials during laser welding, is applied to a case of butt-welded steel sheets having different chemical composition and different thickness. To improve our understanding of influence of thickness ratio on mixing process in the melt pool, numerical results were confronted with elemental maps of welds cross-sections, obtained by EDX analysis.

2. Experimental study

2.1. Experimental design

Welding experiments were conducted between Dual Phase steel (DP) and high manganese steel (TWIP). Elemental composition of steels is provided in the Table 1. TWIP steel sheets were 1.5 mm thick whereas three different thickness of 2, 1.5 and 1 mm of DP sheets were used to produce TWBs with thickness ratios of 0.75, 1 and 1.5. Continuous Yb:YAG laser Trumpf 6002 with beam spot size of 600 µm was focused on top surface of thicker material. Laser power and welding speed were chosen to insure linear welding energy of 0.6 J/m. All combinations between welding speed of 4, 6, 8 and 10 m/min and three laser beam offsets from the joint line (200 µm offset to DP steel, zero offset and 200 µm offset to TWIP steel) were tested. Argon was used as a shielding gas (20 l/min). X-mapping and EDX analysis were performed on two cross-sections per welding condition with Jeol JSM-6610LA field emission SEM equipped with JED-2300 EDX system.

Table 1. Chemical composition and thermal properties of Dual Phase (DP) and high manganese (TWIP) steels.

	C (ωt%)	Mn(ωt%)	Si(ωt%)	Cr(ωt%)	k (W/mK)	T_{fusion} (K)
DP	0.06	1.4	0.2	0.4	35	1800
TWIP	0.66	22.5	0.2	0.1	15	1650

2.2. Average chemical composition of the welds

As TWIP steel contains high manganese concentration, the principal chemical gradient in weld composition is that of Mn. Our previous study (Métais, 2016[a]) showed that distribution of alloying element in the weld reflects the morphology of flow field. Table 2 provides average Mn content found on weld cross-sections.

The mismatch of thermo-physical properties between welded materials influences dilution ratio and thus the mass fraction of Mn in the melted zone. High content of Mn leads to decrease of melting point of TWIP steel comparing to pure iron or DP steel. Moreover, lower heat conductivity explains why the melted zone is wider from TWIP side (under centered beam position).

Welding speed does not produce significant impact on the dilution ratio between steels. Laser beam offset from joint line is a key parameter influencing the dilution ratio. Due to the high difference of manganese content between the DP and TWIP steels, a little shift of laser beam from joint line (< 200 µm) is enough to alter average mass fraction of manganese in the weld from 7 to 20 ωt%. The average Mn content rises with decreasing thickness ratio because TWIP steel has higher Mn concentration. This is also true for other alloying elements, proportionally to the initial gap in composition between base materials.

Table 2. Mn content (ωt%) on weld cross-sections according to EDX analysis.

Thickness ratio	DP thickness	Welding speed	200 µm offset toward DP	No offset	200 µm offset toward TWIP
1.5	2 mm	4 m/min	7	9	17
		6 m/min	7	11	17
		8 m/min	8	14	17
		10 m/min	12	10	15
1	1.5 mm	4 m/min	8	17	18
		6 m/min	11	15	19
		8 m/min	9	13	20
		10 m/min	10	12	13
0.75	1 mm	4 m/min	10	13	19
		6 m/min	10	14	18
		8 m/min	9	10	17
		10 m/min	12	13	18

2.3. Collapse of melted matter

Due to surface tension forces, when thickness ratio is different to one, the melt pool and resulting weld have a geometry smoothed between the two top surfaces instead of a step along joint plane. In fact, surface tension forces minimize the surface energy that impose to the top surface to make an angle of about 45°. This change of cross-section geometry generates particular flows in the top of the weld that influence mixing of melted materials. One third of experiments show a collapse of matter near the top surface (see Figure 1). Melted material from thicker sheet collapses in the melt pool after passage of the keyhole. The keyhole is supposed to have a conical shape with a diameter lower than 600 µm. Thus, farther than 300 µm from the center of laser beam, the steel is melted only by thermal conduction and not by the direct interaction with laser beam. This matter is melted behind the keyhole where the velocity magnitude decreases quickly.

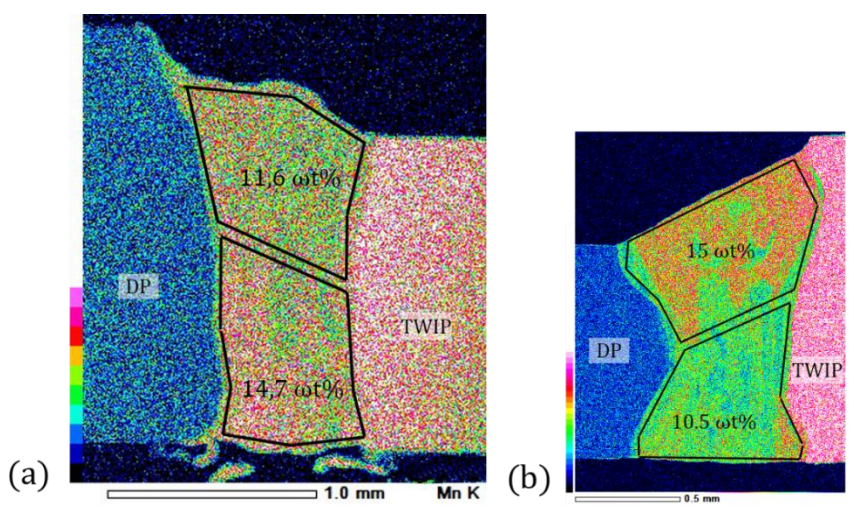

Fig. 1. X-map of Mn distribution on weld cross-section. (a) - DP 2 mm / TWIP 1,5 mm ; 8 m/min ; centered beam position et (b) - DP 1 mm / TWIP 1,5 mm ; 4 m/min ; centered beam position

Because of high cooling rate, melted material does not have enough time for efficient mixing and thus important difference in alloying element content appears between the top and the bottom of the weld. Our previous study on laser welding of high manganese steels (Métais et al., 2016[b]) shows that the phase content of the weld mainly depends on ratio the between carbon and manganese. Metastable Fe-Mn-C diagram (Schumann, 1972) allows predicting the potential formation of brittle martensite phases between TWIP and DP (Figure 2). Two different martensite that exist in this system have different structure: α' martensite (body-centered tetragonal structure) and ε martensite (hexagonal close packed structure). It was found (Métais et al., 2016[b]) that tensile properties of the weld are strongly deteriorated when α' martensite is formed. Based on this metastable diagram, we suppose that the top of the weld of the Figure 1 – (b), where Mn content is around 15 ωt%, is composed of austenite and ε martensite, whereas in the bottom of the weld α' martensite coexist with austenite and ε martensite. For the weld of the Figure 1 – (a), where DP steel is thicker than TWIP steel, the opposite has been found.

Thus, many of our experiments with a gauge difference show an important composition gradient in vertical direction because the top of the weld is mainly composed of material collapsing from the thickest steel sheet. As phase content and tensile properties highly depend on dilution of alloying elements, a homogeneous weld would be better. Numerical simulations need to be used to understand and improve the weldability of dissimilar couple of these steels.

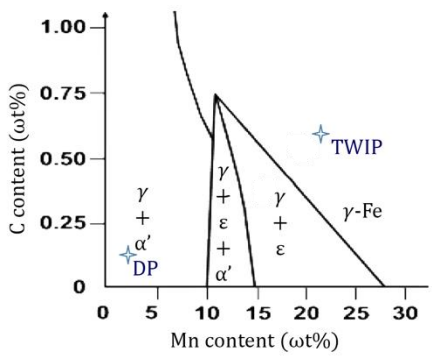

Fig. 2. Metastable phase diagram of Fe-Mn-C system, quenching from 700°C to ambient temperature (Schumann, 1972).

3. Numerical study

3.1. General assumptions

Previously developed 3D model is upgraded to simulate laser butt welding between dissimilar steels with different thicknesses. Detailed mathematical description of the model is available in Métais et al, 2016[a]. Strongly coupled heat transfer, flow and diluted species transport problems are solved with COMSOL Multiphysics® 5.2.

A number of assumptions was made to develop the following tridimensional model in order to reduce the computation time:

- a steady keyhole with a conical geometry;
- heat source as limit condition of temperature inside the keyhole. Temperature is assumed to be uniform $T_{keyhole} = T_{vap}$;

- bottom surface of the weld is assumed to be flat;
- equations are strongly coupled;
- liquid metal is assumed to be Newtonian and incompressible;
- quasi-steady approach is used.

The material properties are defined as functions of temperature and manganese concentration. Smoothed Heaviside step functions are employed to smooth sharp changes of material properties at the boundary of dissimilar metals and in the phase change zone. Macroscopic fluid flows are simulated by taking in consideration the contribution of Marangoni convection, flow around the keyhole, plume shear stress and turbulence (k- ω model). Alloying elements transport is described by Fick equation taking in account convective transport and turbulent diffusivity.

3.2. Geometry and mesh

In case of welding with thickness ratio, the assumption that top surface remains flat can no longer be used. A quasi-steady approach imposes to know the final state of weld surface because free surface problem is not solved. Thus, the top surface of the weld is supposed to be inclined and to pass through the boundaries of melted zone (Figure 3). The geometry is meshed with hexahedral elements of 60 µm except the region that cannot meshed with this kind of element. Around the keyhole and near the complex top surface, tetrahedral elements are used to discretize the geometry.

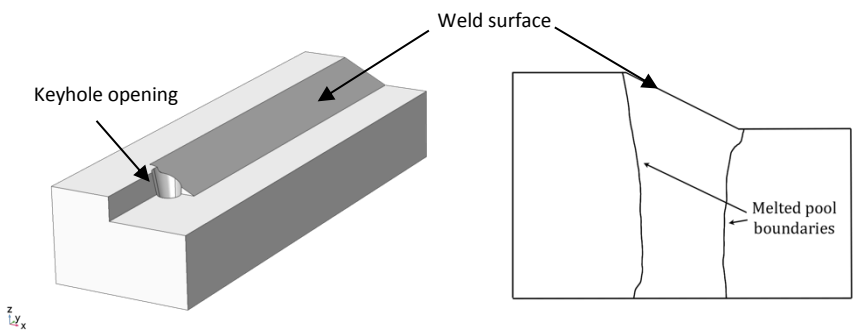

Fig. 3. Tridimensional geometry. Top surface minimized between melt pool boundaries

3.3. Numerical results

Element distribution plays a major role in microstructure and mechanical properties of the joints. The challenge in modelling is to validate numerical flow field with help of experimental observations. Post-mortem X-mapping of alloying element (here, Mn) is used to conclude on matter transport mechanisms. Figure 4 shows an interesting comparison between experimental data and simulation results. One comparison is given for each thickness ratio. It can be seen that the average content in manganese increases with decrease of DP thickness (Figure 4, c,e). Due to quite big mesh size used in simulation, numerical results are smooth compared to experimental data. This model was initially developed for welding of steel plates having same thickness. However, comparison of experimental and numerical results shows that weld geometry and global Mn distribution are well described in case of welding with gauge difference. Present numerical model is a complete tool offering a great potential to improve our understanding of mixing of alloying elements in the melted zone. Nevertheless, the experimental observations show a high variation in element distribution. Two kinds of results have been observed: relatively homogenous element distribution or chemical inhomogeneity due to the collapse of melted matter from thicker sheet. Indeed, the welds on Figure 5 (a,c) show a collapse of TWIP steel on the top surface whereas efficient mixing of manganese is observed in the welds on Figure 5 (b,d). Numerical modelling could be used to study variation in welding parameters and potentially explain why dispersive results are observed experimentally.

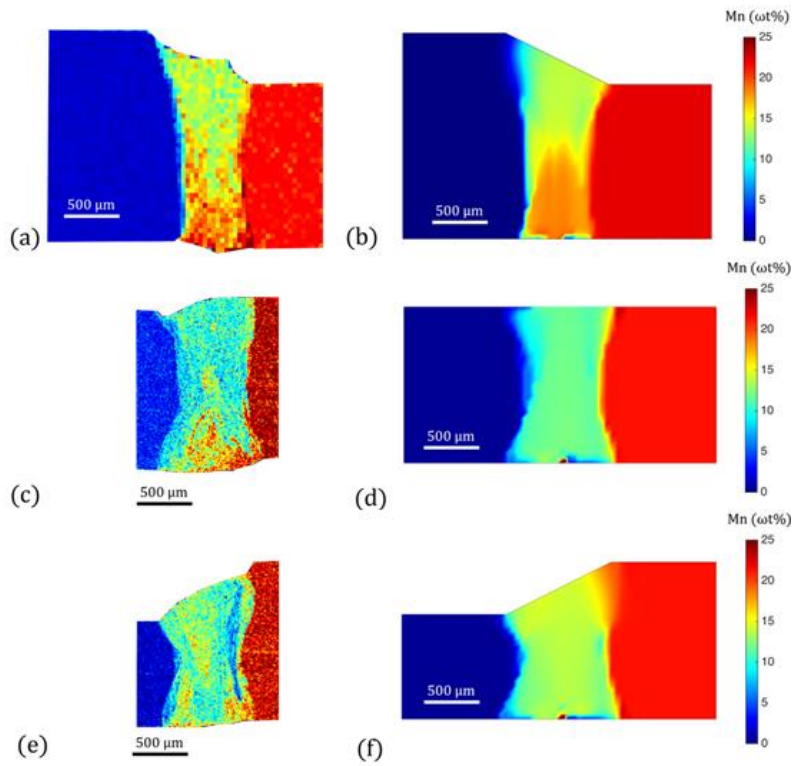

Fig. 4. Experimental (left) and calculated (right) Mn maps (ωt%) of several welds: (a-b) DP 2 mm/TWIP 1.5 mm, 200 µm laser beam shift on TWIP, (c-d) DP 1.5 mm/TWIP 1.5 mm, centered laser beam, (e-f) DP 1 mm/TWIP 1.5 mm centered laser beam (welding speed 6 m/min).

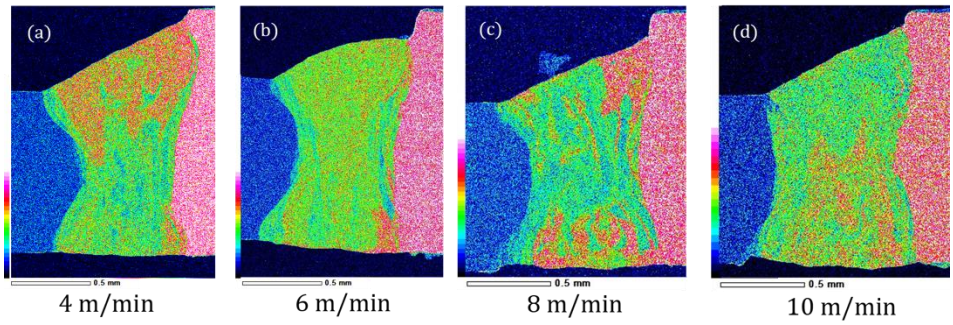

Fig. 5. Post-mortem EDX-mapping of manganese element for different welding speed (DP 2 mm / TWIP 1,5 mm ; centered laser beam)

4. Conclusion

Dissimilar laser welding in butt configuration is a challenge due to the complex mixing of melted materials. A new difficulty appears when welded plates have different thickness. One third of examined weld cross-sections presents important gradient of Mn in vertical direction due to collapse of melted matter from thicker material. The variation of welding speed makes no significant influence on matter collapse, and laser beam offset was identified as a key parameter that determines the concentration of alloying element in melted zone.

Numerical simulation of laser welding was used to provide better understanding of diffusive-convective mixing of alloying elements. Previously developed 3D model of full laser welding between dissimilar materials was applied to case of dissimilar welding with different thickness ratio. It provides good approximation of weld geometry and macroscopic mapping of alloying element. The precision of this model is limited by numerical resources, which impose to work with mesh size that is bigger than observed solidification structures.

References

Métais, A., Matteï, S., Tomashchuk, I., Gaied, S., 2016[a]. Multiphysical Modeling of Transport Phenomena During Laser Welding of Dissimilar Steels, Physics Procedia, vol. 83, pp. 1387 - 1396.

Métais, A., Matteï, S., Tomashchuk, I., Cicala, E., Gaied, S., 2016[b]. Dissimilar steels laser welding: experimental and numerical assesment of weld mixing, ICALEO. San Diego, California, paper #408.

Safdarian Korouyeh, R., Moslemi Naeini, H., Torkamany, M., Liaghat, G., 2013. Experimental and theoretical investigation of thickness ratio effect on the formability of tailor welded blank, Optics & Laser Technology, vol. 51, pp. 24 - 31.

Schumann, H., 1972. Distribution of phases in Fe-Mn-C system after defromation, vol. 17, pp. 605-609.

Seto, A., Yamamoto, T., Niwa, T., 2007. Influences of loading direction and thickness ratio on fatigue properties of tailored welded blanks, International Journal of Fatigue, vol. 29, no. 4, pp. 729 – 737.

Song, Y., Hua, L., 2014. Influences of Thickness Ratio of Base Sheets on Formability of Tailor Welded Blanks, Procedia Engineering, vol. 81, pp. 730 - 735.